

Global Compression Commander: Plug-and-Play Inference Acceleration for High-Resolution Large Vision-Language Models

Xuyang Liu^{1*}, Ziming Wang², Yuhang Han³, Yingyao Wang², Jiale Yuan², Jun Song²[✉],
Bo Zheng², Linfeng Zhang⁴, Siteng Huang⁵, Honggang Chen¹[✉]
¹ Sichuan Univeristy, ² Taobao & Tmall Group of Alibaba, ³ Independant Researcher,
⁴ Shanghai Jiao Tong University, ⁵ Zhejiang University

Abstract

Large vision-language models (LVLMs) excel at visual understanding and reasoning, but face efficiency challenges due to quadratic complexity in processing long multimodal contexts. While token compression techniques can reduce computational costs, existing approaches are designed for single-view LVLMs and fail to consider the unique multi-view characteristics of recent high-resolution LVLMs with dynamic tiling. While existing methods treat all tokens uniformly, our analysis reveals that global thumbnails can naturally guide the compression of local crops by providing holistic context for informativeness evaluation. In this paper, we first analyze dynamic tiling strategy comprehensively, revealing both the complementary nature between thumbnails and crops, and the distinctive characteristics across different crops. Based on our observations, we propose “Global Compression Commander” (i.e., **GlobalCom²**), a novel plug-and-play token compression framework for HR-LVLMs. **GlobalCom²** leverages thumbnail as the “commander” to guide the compression process of local crops, adaptively preserving informative details while eliminating redundancy. Extensive experiments show that **GlobalCom²** maintains over **90%** performance while compressing **90%** visual tokens, reducing FLOPs and peak memory to **9.1%** and **60%** respectively across multiple benchmarks. Our code is available at <https://github.com/xuyang-liu16/GlobalCom2>.

1. Introduction

By bridging visual encoders with Large Language Models (LLMs) [1, 35, 40], Large Vision-Language Models (LVLMs) [2, 24, 27, 28, 51] have achieved remarkable

*Work done during internship at Taobao & Tmall Group of Alibaba.

✉ Corresponding author.



Figure 1. Design philosophy of “global-to-local” guided token compression. **GlobalCom²** evaluates the *information richness* of crops from a global perspective to preserve informative regions while removing redundancy.

progress in multiple tasks. However, the large number of visual tokens leads to prohibitively expensive computation during inference [8, 13, 18, 38], especially for high-resolution images, limiting LVLMs’ practical applications.

To tackle the challenge of inference speed in LVLMs, researchers have primarily focused on model-centric approaches like knowledge distillation [4] and quantization [43], which typically require model retraining, consuming substantial computational resources thus limiting their practical applicability. Recent efforts have shifted towards *data-centric* approaches, exemplified by token compression methods [5, 16, 31, 38, 47], which consider the redundancy in LVLMs’ input visual signals to enhance inference speed by reducing processed tokens while preserving essential information. Most of these methods are architecture-agnostic and training-free, achieving optimal efficiency-accuracy trade-off while being complementary to model-centric approaches [8, 52, 53].

However, current token compression methods were de-

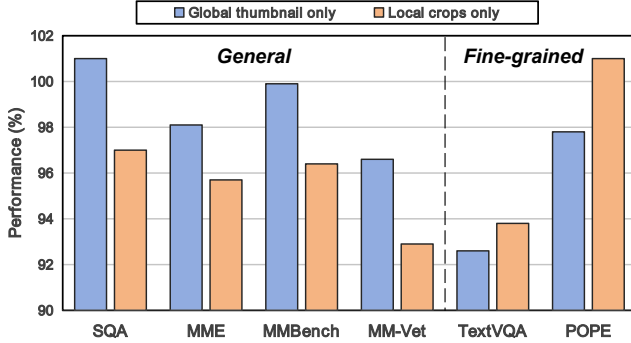


Figure 2. **Effects of global thumbnail and local crops.** Performance (%) denotes relative scores vs. vanilla LLaVA-NeXT-7B.

signed for LVLMs processing *single-view* images (entire image without crop decomposition, as shown in Figure 1 top). With growing demand for high-resolution image understanding, advanced HR-LVLMs like LLaVA-NeXT [29] and InternVL 1.5 [9] adopt dynamic tiling, which divides an image into several crops encoded individually and concatenated with tokens from a global thumbnail (in Figure 1 top). While this *multi-view* approach enables more comprehensive visual understanding, it further increases the number of visual tokens and computational overhead.

Directly applying existing token compression methods to all views might seem straightforward, but such *uniform* compression overlooks two critical structural properties revealed by our analysis: (1) The inherent role of global thumbnails in extracting holistic context and guiding general vision understanding, demonstrated in Figure 2, and (2) The information richness disparity across crops quantified in Figure 3 (e.g., 2.4% average performance gap between discarding most/least informative crops). These oversights lead to *over-compression* of information-rich regions and disrupted visual-semantic hierarchy (see Figure 6).

To establish theoretically grounded compression principles for dynamic tiling-based HR-LVLMs, we first conduct systematic analysis to investigate the roles of global thumbnails and local crops in HR-LVLM image understanding capabilities. Through extensive empirical studies, we identify **two key observations** for token compression: ❶ Visual tokens from thumbnails and crops serve complementary roles - thumbnail tokens capture holistic context while local crop tokens offer fine-grained details, enabling thumbnails to guide holistic token importance evaluation from a global perspective. ❷ Through global context, visual tokens from different crops exhibit varying degrees of informativeness and visual redundancy, necessitating differentiated compression intensity to minimize information loss.

Building on these observations, we propose “**Global Compression Commander**” (i.e., **GlobalCom²**), which follows a “*global-to-local*” guided token compression design philosophy, tailored for HR-LVLMs with dynamic tiling

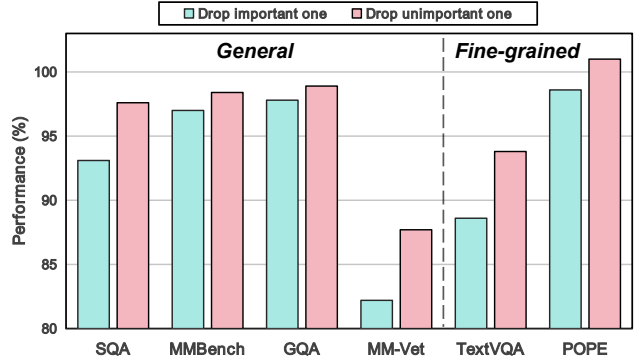


Figure 3. **Effects of different local crops.** Crop importance is quantified through accumulating attention scores between thumbnail patches and the [CLS] token within each crop region.

strategy. As shown in Figure 1, GlobalCom² first leverages holistic information from global thumbnail perspective to evaluate the information richness of each crop, adaptively allocating compression budgets across different crops. It then performs token compression for local crops through comprehensive token evaluation from both global and local perspectives, achieving differentiated compression degrees across regions. Through this “global-to-local” design, GlobalCom² achieves training-free adaptive token compression, which selectively preserves significant visual information while removing redundancy at both global and local perspectives for HR-LVLMs with dynamic tiling.

To summarize, our main contributions are three-fold:

- We empirically analyze the hierarchical nature of dynamic tiling strategy by demonstrating the distinct and complementary roles between thumbnails and crops, as well as the inherent characteristics among local crops, leading to two key observations for token compression.
- We propose a “global-to-local” guided token compression framework GlobalCom², which adaptively adjusts compression intensity based on crops’ information richness and preserves semantically important tokens with fine-grained details across the entire image.
- Extensive experiments on LLaVA-NeXT and LLaVA-OneVision demonstrate superior efficiency-performance trade-offs, maintaining 90% performance with 90% token reduction, while achieving substantial memory savings and throughput improvement.

2. Related Work

2.1. High-resolution LVLMs

LVLMs generally combine a vision encoder and a large language model (LLM) decoder, bridged by a visual projector that maps visual features into the LLM’s embedding space. Representative works include BLIP-2 [22] which utilizes a Q-Former as the visual projector, and LLaVA-1.5 [28] which employs a multi-layer perceptron (MLP) projector to

integrate visual and textual information.

Previous LVLMs [2, 28] resize images to a fixed resolution before processing, which often leads to shape distortion and loss of local details in high-resolution images. To address this, a series of LVLMs have been proposed to handle high-resolution images, which can be categorized into three groups: (1) Hybrid resolution methods using dual visual encoders, represented by Mini-Gemini [24] and LLaVA-HR [34]. (2) Native resolution methods adopting NaViT-style [11] encoders, represented by Qwen2-VL [42]. (3) Dynamic tiling methods, represented by LLaVA-NeXT [29] and InternVL-1.5 [9], which split images into regions and process them with a single encoder. Due to its efficiency and effectiveness in vision encoding, dynamic tiling has been widely adopted in subsequent works [6, 21, 30].

While increasing local visual tokens enhances detail recognition and hallucination suppression, it also introduces computational challenges in inference speed and memory usage. In this work, we focus on improving the efficiency of dynamic tiling-based HR-LVLMs.

2.2. Token Compression for LVLMs

Token compression, which aims to reduce the sequence length of tokens for computation efficiency, has been widely adopted for model acceleration [3, 25, 37]. For LVLMs, recent works have focused on training-free token compression paradigms, which can be broadly categorized into two streams: (1) Token compression during Vision Encoding stage [16, 38, 45]: For example, FasterVLM [52] utilizes [CLS] attention scores from the visual encoder to re-rank and retain top visual tokens. (2) Token compression during LLM Decoding stage [8, 26, 46]: Representative works include FastV [8], which prunes tokens based on self-attention scores in LLM, and SparseVLM [53], which adaptively prunes visual tokens based on their attention scores with text tokens. However, when applying these methods to HR-LVLMs with dynamic tiling, they treat all visual tokens with uniform compression strategies, overlooking the distinct roles of global thumbnail and local crop tokens in image understanding for HR-LVLMs.

In this paper, unlike existing token compression methods, we propose a “global-to-local” guided compression strategy that leverages global thumbnail as a “commander” to guide token compression in HR-LVLMs.

3. Analysis of HR-LVLM with Dynamic Tiling

3.1. Preliminary

We take LLaVA-NeXT [29], a widely-adopted HR-LVLM with dynamic tiling, as an example to conduct our analysis.

Model Architecture. Given the input image and textual instructions, LLaVA-NeXT generates instruction-following responses in an autoregressive manner through two stages:

- **Vision Encoding:** LLaVA-NeXT adopts CLIP-ViT [36] to transform raw pixels into unified visual representations, followed by a two-layer MLP Projector that aligns visual embeddings with the language embedding space.
- **LLM Decoding:** The decoder-only LLM takes concatenated image and prompt tokens as input and decodes them through next-token prediction to generate responses.

Dynamic Tiling Input Pre-processing. LLaVA-NeXT processes arbitrary-resolution images through adaptive dynamic cropping using seven grid templates: $\{2 \times 2, 1 \times \{2, 3, 4\}, \{2, 3, 4\} \times 1\}$. For an input image of size $W \times H$, it is scaled to $(336 \times a) \times (336 \times b)$ based on the selected template, producing $n = a \times b$ local crops \mathbf{X}^L of size 336×336 (with padding if necessary) and a thumbnail \mathbf{X}^G . With N tokens per crop, the total token length is $(1 + n) \times N$.

Visual Tokens Post-processing. Following [28], LLaVA-NeXT removes padding tokens and uses special tokens to mark image boundaries, preserving aspect ratio information while improving efficiency.

3.2. Stepping into Dynamic Tiling Mechanism

HR-LVLMs process high-resolution images using dynamic tiling with thumbnails and crops. We analyze their characteristics to guide token compression design.

(I) Functions of Thumbnail and Crops. We begin with an exploratory experiment to investigate how thumbnail and crops contribute to image understanding in HR-LVLMs by using them separately as input to LLaVA-NeXT-7B model.

As shown in Figure 2, using global thumbnail alone yields superior performance on general visual perception benchmarks such as SQA [33], MME [12], MMBench [32], and MM-Vet [48]. This advantage stems from global thumbnails providing holistic visual information through complete ViT encoding. In contrast, using only local crops, where ViT independently encodes each crop, shows inferior performance on these general visual perception tasks. However, local crops excel in fine-grained perception tasks like TextVQA [39] (VQA^T, testing text-centric visual understanding) and POPE [23] (testing model hallucination) by providing detailed features. Therefore, we identify that:

Observation 1: Global thumbnails and local crops serve *complementary functions* in HR-LVLMs with dynamic tiling: the former acts as a “comprehensive visual extractor” for holistic representations, while the latter serves as a “detailed visual capturer” for fine-grained representations.

(II) Information Richness in Different Crops. Given that dynamic tiling leads to distinct visual representations across crops, we investigate the variance through both qualitative and quantitative perspectives.

Through visual inspection of input image in Figure 4, we observe that the upper two crops contain significant visual content (e.g., football players), while the lower two

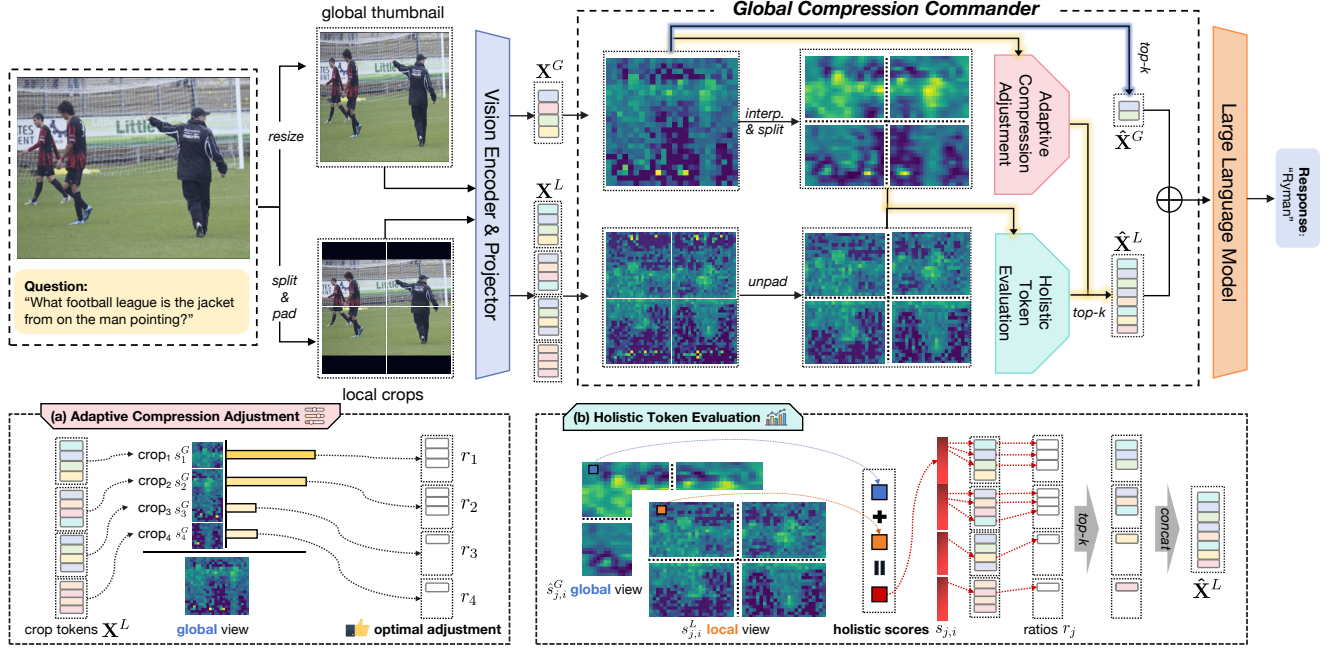


Figure 4. **Overall framework of GlobalCom²**. GlobalCom² guides token compression for HR-LVLMs through: 1) compressing thumbnail tokens (blue path); and 2) compressing crop tokens (yellow paths) by: (a) adaptively adjusting compression intensity based on visual information richness at global view, and (b) performing compression according to token informativeness at global and local views.

crops exhibit considerable visual redundancy (predominantly grass areas). To quantitatively validate this observed variation in informational content, we leverage insights from previous works [16, 25], which demonstrated that attention scores between [CLS] and patch tokens effectively reflect token importance. As shown in the upper middle of Figure 4, our visualization of attention scores between patch tokens and the [CLS] token from CLIP-ViT’s last layer reveals notably higher attention values in the upper regions, confirming richer semantic information in upper crops from a global perspective.

Building upon this qualitative analysis, we conduct quantitative studies to validate our observations. Since attention scores with the [CLS] token effectively measure token-level semantic richness, we leverage these scores to assess crop importance by computing the sum of partitioned attention scores within each crop region. To examine crop contributions in HR-LVLMs, we conduct experiments on LLaVA-NeXT-7B by selectively dropping local crops (*i.e.*, dropping the most/least important one). As shown in Figure 3, dropping the most versus least important crops leads to significant performance gaps across visual understanding tasks, with an average drop of **2.4%** across six benchmarks and particularly notable in VQA^T (**5.2%** gap). Based on the above analysis, we identify that:

Observation 2: Local crops exhibit *varying information richness*, leading to different contributions to the overall visual understanding of HR-LVLMs with dynamic tiling,

with visually informative crops being particularly crucial for capturing fine-grained local details.

4. Global Compression Commander

As discussed in Section 3, HR-LVLMs’ dynamic tiling strategy leads to significant token length increase (**5 \times** in LLaVA-NeXT [29], **10 \times** in LLaVA-OneVision [21]), where the quadratic complexity of self-attention [41] becomes a major bottleneck. To address this challenge, we aim to directly improve HR-LVLMs’ inference speed through visual token compression, as illustrated in Figure 4.

Motivated by observation 1 in Section 3.2 that global thumbnail serves as a “comprehensive visual extractor” providing visual representations from a holistic perspective, we leverage it as a “**Global Compression Commander**” (GlobalCom²) to guide token compression for HR-LVLMs, as illustrated in Figure 4. In what follows, we first elaborate on how our GlobalCom² guides token compression for the global thumbnail.

Since visual token compression aims to preserve informative tokens while eliminating redundant representations in visual content, the key for global thumbnails lies in identifying tokens that capture essential holistic information. Given that the [CLS] token serves as an effective global image representation [16, 25], GlobalCom² leverages the last ViT layer’s attention map to compute average attention between each global thumbnail token and the [CLS] token (blue path in Figure 4). Specifically, for 1D token sequence

\mathbf{X}^G of length N in the global thumbnail, the importance score s_i^G for the i -th token is:

$$s_i^G = \frac{\exp(\mathbf{q}^{\text{CLS}} \mathbf{K}_i^\top / \sqrt{D})}{\sum_{i=1}^N \exp(\mathbf{q}^{\text{CLS}} \mathbf{K}_i^\top / \sqrt{D})}, \quad (1)$$

where \mathbf{q}^{CLS} and $\mathbf{K} \in \mathbb{R}^{N \times D}$ are query of [CLS] and keys of \mathbf{X}^G . Based on these scores, tokens with higher s^G capture richer semantic information and should be preserved. Given a preset token retention ratio R (%), GlobalCom² preserves the top- k ($k = R \times N$) tokens ranked by s^G :

$$\mathbf{X}^G \rightarrow \hat{\mathbf{X}}^G = \text{TopK}(\mathbf{X}^G, s^G, R \times N) \quad (2)$$

where $\hat{\mathbf{X}}^G$ is the compressed thumbnail sequence. This training-free compression mechanism reduces computational cost by preserving only the informative tokens.

Due to dynamic tiling’s multi-partitioning process, local crops produce multiple independent token sequences containing distinct visual contents, with each crop exhibiting different levels of redundancy and collectively leading to longer sequences compared to the global thumbnail. Inspired by observation ②, local crops with different semantic richness warrant different token compression degrees. Specifically, semantically rich crops should retain more tokens to preserve crucial local details, while less informative ones can be more aggressively compressed to help LLMs focus on informative visual signals.

To implement such adaptive compression, motivated by observations ①-②, we aim to guide the token compression of local crops from a global perspective. Specifically, GlobalCom² employs two aspects of global guidance: (a) Adaptive Compression Adjustment that dynamically adapts compression intensity for each crop based on its information richness, and (b) Holistic Token Evaluation that assesses token informativeness from both local and global perspectives. We detail these two global guidance below.

4.1. Adaptive Compression Adjustment

As presented in the bottom-left of Figure 4, GlobalCom² first analyzes the semantic contribution of each local crop to the overall visual information, and accordingly applies adaptive token compression at different levels.

To achieve differentiated token compression for local crops, GlobalCom² adaptively adjusts the compression degrees for each crop based on its informativeness. Specifically, for the j -th crop, we define its *information richness score* s_j^G from the global perspective by accumulating patch-to-[CLS] attention scores over its corresponding region in the global thumbnail: $s_j^G = \sum_{i \in \text{crop}_j} s_i^G$, where s_i^G denotes the *informativeness score* of each token in the crop region from the thumbnail. To stabilize s_j^G , we compute $\tilde{s}_j = (s_j^G - \max(s_j^G)) / \tau$ with a temperature parameter $\tau = 10$, and then compute the relative importance weight

σ_j of the j -th crop via softmax across all n crops:

$$\sigma_j = \frac{\exp(\tilde{s}_j)}{\sum_{l=1}^n \exp(\tilde{s}_l) + \epsilon}, \quad (3)$$

where $\epsilon = 10^{-8}$ prevents division by zero. Finally, we adjust the preset retention ratio R (%) according to the computed importance weight σ_j . This adjustment ensures crops with higher importance preserve more tokens while maintaining the average retention ratio:

$$r_j = R \times \left(1 + \sigma_j - \frac{1}{n}\right), \quad (4)$$

where $\sigma_j - \frac{1}{n}$ represents the relative deviation from average importance, leading to more aggressive compression for less important regions (values exceeding 100% are capped).

To this end, GlobalCom² optimally allocates compression degrees (*i.e.*, $\{r_1, r_2, r_3, r_4\}$ in Figure 4) based on each crop’s information richness from global view, enabling differentiated token compression degrees across crops.

4.2. Holistic Token Evaluation

After determining the optimal compression budgets, GlobalCom² evaluates the importance of tokens within each crop and preserves the essential ones, as shown in the bottom-right of Figure 4.

After independent ViT encoding of each local crop, the attention values between patch tokens and the [CLS] token in its corresponding attention map reflect each token’s semantic importance within the crop. Similar to global analysis, GlobalCom² computes a set of *local importance scores* $\{s_j^L\}_{j=1}^n$, where $s_{j,i}^L$ denotes the score of the i -th token in the j -th crop based on its own final-layer attention map. Here, each s_j^L represents the attention scores after excluding padding tokens. However, since local crops are encoded independently during vision encoding stage, these local scores only reflect token importance within individual crops, failing to capture their significance in the full image context. This *local-only* evaluation poses a potential challenge, as semantically crucial elements that bridge different image regions might be overlooked.

Motivated by observation ① that global thumbnails provide holistic visual representations, GlobalCom² extends local token evaluation with global context to achieve more comprehensive importance assessment. As shown in Figure 4, GlobalCom² reshapes the 1D attention scores s^G of \mathbf{X}^G into 2D format and bilinearly interpolates them to match the original image dimensions (denoted as “*interp.*”), yielding $\hat{s}^G \in \mathbb{R}^{H \times W}$. Subsequently, \hat{s}^G is split into n sub-attention maps $\{\hat{s}_j^G\}_{j=1}^n$ according to the local crop partitioning, where these sub-attention maps measure the semantic significance of tokens in local crops from a global perspective. Combining sub-attention maps $\{\hat{s}_j^G\}_{j=1}^n$ with the local importance scores $\{s_j^L\}_{j=1}^n$, GlobalCom² is able

to comprehensively evaluate token importance from both global and local perspectives.

Specifically, both global sub-attention maps $\{\hat{s}_j^G\}_{j=1}^n$ and local attention scores $\{s_j^L\}_{j=1}^n$ are first L2-normalized. The *holistic score* $s_{j,i}$ for the i -th token in the j -th local crop is then calculated by integrating its normalized *global importance score* $\hat{s}_{j,i}^G$ and *local importance score* $s_{j,i}^L$ as:

$$s_{j,i} = \alpha \hat{s}_{j,i}^G + (1 - \alpha) s_{j,i}^L \quad (5)$$

Here, $\alpha \in [0, 1]$ balances the two importance scores, defaulting to 0.5 for equal weighting. Based on the *holistic scores*, the token compression process for each local crop can be formulated as:

$$\mathbf{X}_j^L \rightarrow \hat{\mathbf{X}}_j^L = \text{TopK}(\mathbf{X}_j^L, s_j, r_j \times N) \quad (6)$$

where $\{\hat{\mathbf{X}}_j^L\}_{j=1}^n$ represents the compressed token sequences. Through holistic token evaluation, GlobalCom² identifies tokens that are significant in global context while preserving local details, providing fine-grained visual information for LLM. See Appendix 11 for algorithm details.

4.3. GlobalCom² without [CLS] Token

For HR-LVLMs without [CLS] token (e.g., LLaVA-OneVision [21] with SigLIP [50]), we propose an alternative token informativeness measure for GlobalCom². Specifically, given a sequence of vision tokens $\mathbf{X} \in \mathbb{R}^{N \times d}$ after vision encoding (both thumbnail and crops), we first compute a global mean vector $\mathbf{g} \in \mathbb{R}^d$ through global average pooling over all tokens, and then calculate the cosine similarity between each patch token \mathbf{x}_i and \mathbf{g} :

$$c_i = \cos(\mathbf{x}_i, \mathbf{g}) = \frac{\mathbf{x}_i \cdot \mathbf{g}}{\|\mathbf{x}_i\| \|\mathbf{g}\|}, \quad (7)$$

The informativeness score $s_i = -c_i$ is negatively correlated with the similarity, reflecting that tokens with greater difference from \mathbf{g} carry more unique information. Specifically, tokens exhibiting low similarity to \mathbf{g} represent distinctive and irreplaceable visual elements, while highly similar tokens typically correspond to redundant or common patterns. This scoring mechanism serves as an effective alternative to [CLS]-based scoring in Eq. (2)-Eq. (5) for models without [CLS] token. It is adopted to evaluate both crop-level information richness and token-level importance in LLaVA-OneVision. We conduct comprehensive quantitative and qualitative analyses in Appendix 8 to explore how to measure token informativeness without [CLS] token.

5. Experiments

5.1. Experimental Setting

Benchmark Details. We evaluate GlobalCom² on various multimodal benchmarks including: VQAv2 [14], GQA [17], VizWiz [15], SQA [33], VQA^T [39], AI2D [19],

MMStar [7], MME [12], MMBench [32], MMBench-CN [32], MM-Vet [48], and SEED-Bench [20].

Implementation Details. We select two representative HR-LVLMs with dynamic tiling: LLaVA-NeXT [29] and LLaVA-OneVision [21] to evaluate the effects of our GlobalCom². For hyper-parameters, τ and α are respectively set as 10 and 0.5 for benchmark evaluations. More implementation details are provided in the Appendix 9.

Comparison Details. We compare GlobalCom² with FastV [8], SparseVLM [53], and FasterVLM [52] at different retention ratios R (75%, 50%, 25%, 10%). While FastV and SparseVLM compress from the default 2880 tokens, FasterVLM and our method first unpad the token sequences - resulting in fewer preserved tokens given the same R .

5.2. Main Results

Results on LLaVA-NeXT. Table 1 compares GlobalCom² with existing methods on 10 benchmarks using LLaVA-NeXT at different retention ratios. **(1)** GlobalCom² outperforms baselines across most benchmarks, maintaining **>90%** of original performance at all retention ratios. Notably, GlobalCom² even surpasses the original model on several benchmarks (MMB, MME, POPE) even at 50% retention, suggesting effective preservation of semantically crucial tokens for visual understanding. **(2)** GlobalCom² excels at **low retention ratios** (25% and 10%), surpassing FastV and SparseVLM by 4.2% and 8.6% respectively at 10% retention. On VQA^T, our method maintains stable performance while others degrade significantly (e.g., SparseVLM drops 12.9%), demonstrating its effectiveness in fine-grained visual understanding. **(3)** GlobalCom² demonstrates effective hallucination mitigation on POPE, even surpassing the original model. While text-guided methods (*i.e.*, FastV and SparseVLM) consistently show hallucination issues, vision-semantic approaches (*i.e.*, our GlobalCom² and FasterVLM) better preserve crucial visual details by avoiding over-reliance on instructions.

Results on LLaVA-OneVision. Figure 5 further presents GlobalCom²'s performance across benchmarks under varying retention ratios R on LLaVA-OneVision. Generally, model performance correlates with R , with more aggressive compression leading to degradation. Vision-centric tasks (*e.g.*, GQA, VizWiz, MME, SEED) show substantial drops with reduced visual tokens, while SQA maintains robust performance even with minimal tokens, suggesting language understanding dominates in scientific reasoning. Notably, GlobalCom² preserves **90.5%** performance at $R = 10\%$ while consuming only **35.4%** of the original GPU memory, all without any training overhead, demonstrating its effective and efficient token compression.

Method	VQA _{v2}	GQA	VizWiz	SQA	VQA ^T	POPE	MME	MMB	MMBCN	MM-Vet	Average
<i>Upper Bound, 2880 Tokens</i>											
LLaVA-NeXT-7B [29]	81.8	64.2	57.6	70.1	64.9	86.5	1519.0	67.4	60.6	43.9	100.0%
<i>Ratio=75%, Retain up to 2160 Tokens</i>											
FastV [8]	81.1	62.5	55.1	69.3	59.7	86.3	1506.3	67.6	59.0	41.7	97.5%
SparseVLM [53]	81.1	62.6	55.2	68.5	60.3	73.2	1507.8	66.1	58.6	41.9	95.7%
FasterVLM [52]	81.1	63.7	56.5	68.4	59.1	87.5	1533.4	67.5	60.2	38.5	97.4%
GlobalCom²	81.3	63.8	56.5	68.7	62.5	87.8	1548.4	68.0	60.6	40.6	98.8%
<i>Ratio=50%, Retain up to 1440 Tokens</i>											
FastV [8]	80.7	61.8	54.9	69.1	59.6	85.5	1490.3	67.4	58.5	41.2	96.8%
SparseVLM [53]	80.9	62.0	55.7	68.1	60.0	73.4	1484.9	65.7	58.9	39.9	95.0%
FasterVLM [52]	80.6	63.4	56.4	69.1	58.9	87.7	1533.3	67.4	60.4	39.6	97.7%
GlobalCom²	80.6	63.9	56.5	68.5	62.3	88.1	1552.9	67.6	60.5	40.4	98.6%
<i>Ratio=25%, Retain up to 720 Tokens</i>											
FastV [8]	78.9	60.4	54.2	69.8	58.4	83.1	1477.3	65.6	57.0	41.1	95.3%
SparseVLM [53]	78.9	60.9	55.6	67.5	58.1	71.0	1446.1	63.8	57.0	38.0	92.6%
FasterVLM [52]	78.3	61.3	55.4	67.1	58.8	87.2	1454.6	66.0	58.4	37.8	95.1%
GlobalCom²	79.4	61.4	55.7	68.1	60.9	87.6	1493.5	65.9	58.0	40.7	96.6%
<i>Ratio=10%, Retain up to 288 Tokens</i>											
FastV [8]	71.9	55.9	53.1	69.3	55.7	71.7	1282.9	61.6	51.9	33.7	87.3%
SparseVLM [53]	71.6	56.1	53.2	68.6	52.0	63.2	1332.2	54.5	50.7	24.7	82.7%
FasterVLM [52]	74.0	56.9	52.6	66.5	56.5	83.6	1359.2	61.6	53.5	35.0	89.8%
GlobalCom²	76.7	57.1	54.6	68.7	58.4	83.8	1365.5	61.8	53.4	36.4	91.5%

Table 1. Comparison with other training-free LVLm token compression methods with LLaVA-NeXT across 10 benchmarks. ‘‘Average’’ shows the mean performance across 10 benchmarks at different retention ratios (75% to 10%), with best results highlighted.

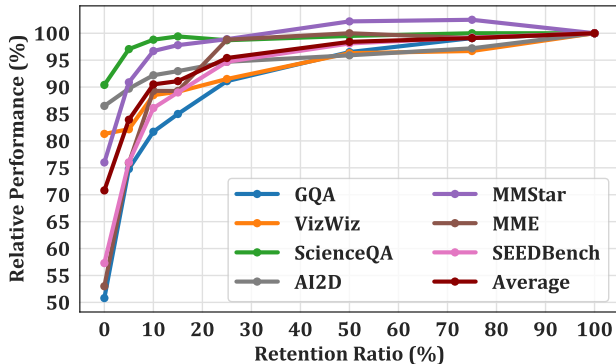


Figure 5. Results of GlobalCom² on LLaVA-OneVision.

5.3. Ablation Study and Analysis

We conduct ablation studies on GlobalCom² with $R = 25\%$ across five benchmarks (VQA^T, POPE, MME, SQA and MM-Vet) covering various vision-language tasks.

Ablation on Adaptive Compression Adjustment for Local Crops. Table 2 compares different compression adjustment strategies: (a) ‘‘Uniform’’, a uniform strategy with fixed 25% token retention across all crops serving as our baseline, and three adaptive strategies - (b) ‘‘n_{top-k}’’, which adjusts compression degrees based on the proportion of thumbnail’s top- k ($k = 25\% \times N$) most informative tokens present in each crop region, (c) ‘‘Softmax (max)’’, which applies softmax normalization over the maximum token im-

Method	VQA ^T	POPE	MME	SQA	MM-Vet	Avg.
<i>Upper Bound, 2880 Tokens</i>						
Vanilla	64.9	86.5	1519.0	70.1	43.9	100.0%
<i>Ratio=25%, Retain up to 720 Tokens</i>						
Uniform	60.1	87.2	1454.6	67.1	37.8	94.2%
n _{top-k}	59.8	87.3	1471.5	67.4	35.7	94.5%
Softmax (max)	60.3	87.2	1462.6	67.3	38.4	94.7%
Softmax (sum)	60.6	87.4	1473.3	67.6	39.6	95.6%

Table 2. Effects of different compression adjustment strategies.

portance score s_j^G within each crop’s corresponding thumbnail region, and (d) ‘‘Softmax (sum)’’, which computes softmax over the sum of token importance scores s_j^G in each crop’s corresponding thumbnail region.

As shown in Table 2, our adopted ‘‘Softmax (sum)’’ strategy achieves the best performance. Despite ‘‘Uniform’’, the other strategies acknowledge varying importance across crops. However, both n_{top-k} and ‘‘Softmax(max)’’ strategies only consider the strongest visual representation capability within each crop, rather than evaluating the overall importance of the entire crop to the whole image. In contrast, our adopted ‘‘Softmax (sum)’’ strategy dynamically modulates compression intensity according to each crop’s relative importance to the entire image, thereby preserving richer semantic visual information from high-resolution inputs and enabling LLM to better capture fine-grained visual details.

Ablation on Holistic Token Evaluation for Local Crops.

Question1: "What is the brand of this camera?"
 Answer1: "DAKOTA DIGITAL"



Question2: "What brand is this drink?"
 Answer2: "REDHOOK"



Figure 6. **Visualization of token compression.** Row 1 shows input images with thumbnail and crops. Rows 2 and 3 present compressed results from FasterVLM and our GlobalCom² respectively, where grey masks indicate discarded tokens.

Method	VQA ^T	POPE	MME	SQAMM-Vet	Avg.	
<i>Upper Bound, 2880 Tokens</i>						
Vanilla	64.9	86.5	1519.0	70.1	43.9	100.0%
<i>Ratio=25%, Retain up to 720 Tokens</i>						
Local only	60.6	87.4	1473.3	67.6	39.6	95.6%
Global only	60.2	86.4	1488.5	67.9	37.8	94.7%
Global and Local	60.9	87.6	1493.5	68.1	40.7	96.7%

Table 3. **Effects of different token evaluation metrics.**

Table 3 compares different token evaluation strategies for token compression. For the i -th token in crop j , “Global” and “Local” refer to importance scores $\hat{s}_{j,i}^G$ and $\hat{s}_{j,i}^L$ respectively. While both global and local token evaluation strategies are effective, each has its limitations. Local-only evaluation excels at fine-grained tasks (VQA^T, POPE) but underperforms on general perception benchmarks (MME, SQA) due to missing global context. Conversely, global-only evaluation maintains good general perception but may overlook crucial local details. GlobalCom² achieves optimal performance by combining both global and local perspectives, benefiting from their complementary strengths.

5.4. Efficiency Analysis

Table 4 compares inference efficiency among SparseVLM, FasterVLM and our GlobalCom². Unlike SparseVLM which requires explicit attention scores during decoding and is incompatible with FlashAttention [10], FasterVLM and our GlobalCom² enable efficient computation before LLM decoding for efficient computation. As a plug-and-play solution, GlobalCom² achieves superior performance-efficiency trade-offs, maintaining **90%** of the original performance while dramatically reducing peak memory usage by **40%** and boosting inference throughput by **1.8×**. Detailed efficiency analysis can be found in Appendix 10.4.

Method	FLOPs↓ (T)	Memory↓ (GB)	Throughput↑ (samples/s)	Performance↑
<i>Upper Bound, 2880 Tokens</i>				
Vanilla	41.7	23.0	3.8	100%
<i>Ratio=10%, Retain up to 288 Tokens</i>				
SparseVLM	5.4 (↓87.1%)	24.2 (↑5.2%)	5.9 (1.6×)	82.7%
FasterVLM	3.8 (↓90.9%)	13.6 (↓40.1%)	6.7 (1.8×)	89.8%
GlobalCom²	3.8 (↓90.9%)	13.9 (↓40.0%)	6.7 (1.8×)	91.5%

Table 4. **Efficiency comparisons.** “Memory”: peak GPU memory; “Throughput”: POPE samples/second; “Performance”: average score on 10 multimodal benchmarks.

5.5. Visualizations

Figure 6 visualizes token compression on VQA^T, where FasterVLM [52] and our GlobalCom² are compared under aggressive compression ($R = 10\%$). FasterVLM assumes *uniform* information richness across crops and preserves the same ratio of tokens for each local crop, evaluating token importance only from local perspectives. This leads to both information loss and redundancy retention, as evidenced by the redundant camera metal parts preserved in the last two crops of the first case. In contrast, our GlobalCom² adopts a global perspective to assess actual informativeness of each crop and *adaptively* adjusts compression intensity accordingly. This enables our method to preserve crucial visual details while maximizing redundancy removal, achieving 1.9% higher accuracy than FasterVLM on VQA^T under $R = 10\%$. More cases in Appendix 8 show GlobalCom²’s consistent effectiveness in adaptive token preservation across both global and local views.

6. Conclusion

Token compression has achieved significant progress in accelerating LLM inference. When applying existing methods to HR-LVLMs with dynamic tiling strategy, these methods treat global thumbnails and local crops uniformly, over-

looking their inherent characteristics. Through analyzing HR-LVLMs with dynamic tiling, we reveal distinct roles between thumbnails and crops, and observe varying information densities across crops. Based on these findings, we propose GlobalCom², a plug-and-play token compression framework that operates on a “global-to-local” guided principle, adaptively preserves informative regions as well as minimizes redundancy. Experiments show that GlobalCom² achieves superior performance and efficiency, significantly outperforming existing baselines.

References

- [1] Jinze Bai, Shuai Bai, Yunfei Chu, Zeyu Cui, Kai Dang, Xiaodong Deng, Yang Fan, Wenbin Ge, Yu Han, Fei Huang, Binyuan Hui, Luo Ji, Mei Li, Junyang Lin, Runji Lin, Dayiheng Liu, Gao Liu, Chengqiang Lu, Keming Lu, Jianxin Ma, Rui Men, Xingzhang Ren, Xuancheng Ren, Chuanqi Tan, Sinan Tan, Jianhong Tu, Peng Wang, Shijie Wang, Wei Wang, Shengguang Wu, Benfeng Xu, Jin Xu, An Yang, Hao Yang, Jian Yang, Shusheng Yang, Yang Yao, Bowen Yu, Hongyi Yuan, Zheng Yuan, Jianwei Zhang, Xingxuan Zhang, Yichang Zhang, Zhenru Zhang, Chang Zhou, Jingren Zhou, Xiaohuan Zhou, and Tianhang Zhu. Qwen technical report. *arXiv preprint arXiv:2309.16609*, 2023. 1
- [2] Jinze Bai, Shuai Bai, Shusheng Yang, Shijie Wang, Sinan Tan, Peng Wang, Junyang Lin, Chang Zhou, and Jingren Zhou. Qwen-VL: A frontier large vision-language model with versatile abilities. *arXiv preprint arXiv:2308.12966*, 2023. 1, 3
- [3] Daniel Bolya, Cheng-Yang Fu, Xiaoliang Dai, Peizhao Zhang, Christoph Feichtenhofer, and Judy Hoffman. Token merging: Your ViT but faster. In *Proceedings of the International Conference on Learning Representations*, 2023. 3
- [4] Yuxuan Cai, Jiangning Zhang, Haoyang He, Xinwei He, Ao Tong, Zhenye Gan, Chengjie Wang, and Xiang Bai. Llavakd: A framework of distilling multimodal large language models. *arXiv preprint arXiv:2410.16236*, 2024. 1
- [5] Junbum Cha, Wooyoung Kang, Jonghwan Mun, and Byungseok Roh. Honeybee: Locality-enhanced projector for multimodal LLM. In *Proceedings of the IEEE/CVF Conference on Computer Vision and Pattern Recognition*, pages 13817–13827, 2024. 1
- [6] Kezhen Chen, Rahul Thapa, Rahul Chalamala, Ben Athiwaratkun, Shuaiwen Leon Song, and James Zou. Dragonfly: Multi-resolution zoom supercharges large visual-language model. *arXiv preprint arXiv:2406.00977*, 2024. 3
- [7] Lin Chen, Jinsong Li, Xiaoyi Dong, Pan Zhang, Yuhang Zang, Zehui Chen, Haodong Duan, Jiaqi Wang, Yu Qiao, Dahua Lin, and Feng Zhao. Are we on the right way for evaluating large vision-language models? In *Proceedings of the Advances in Neural Information Processing Systems*, 2024. 6, 2
- [8] Liang Chen, Haozhe Zhao, Tianyu Liu, Shuai Bai, Junyang Lin, Chang Zhou, and Baobao Chang. An image is worth 1/2 tokens after layer 2: Plug-and-play inference acceleration for large vision-language models. In *Proceedings of the European Conference on Computer Vision*, 2024. 1, 3, 6, 7, 2
- [9] Zhe Chen, Weiyun Wang, Hao Tian, Shenglong Ye, Zhangwei Gao, Erfei Cui, Wenwen Tong, Kongzhi Hu, Jiapeng Luo, Zheng Ma, Ji Ma, Jiaqi Wang, Xiaoyi Dong, Hang Yan, Hewei Guo, Conghui He, Botian Shi, Zhenjiang Jin, Chao Xu, Bin Wang, Xingjian Wei, Wei Li, Wenjian Zhang, Bo Zhang, Pinlong Cai, Licheng Wen, Xiangchao Yan, Min Dou, Lewei Lu, Xizhou Zhu, Tong Lu, Dahua Lin, Yu Qiao, Jifeng Dai, and Wenhai Wang. How far are we to gpt-4v? closing the gap to commercial multimodal models with open-source suites. *arXiv preprint arXiv:2404.16821*, 2024. 2, 3
- [10] Tri Dao, Daniel Y. Fu, Stefano Ermon, Atri Rudra, and Christopher Ré. Flashattention: Fast and memory-efficient exact attention with io-awareness. In *Proceedings of the Advances in Neural Information Processing Systems*, 2022. 8
- [11] Mostafa Dehghani, Basil Mustafa, Josip Djolonga, Jonathan Heek, Matthias Minderer, Mathilde Caron, Andreas Peter Steiner, Joan Puigcerver, Robert Geirhos, Ibrahim Alabdulmohsin, Avital Oliver, Piotr Padlewski, Alexey A. Gritsenko, Mario Lucic, and Neil Houlsby. Patch n’ pack: Navit, a vision transformer for any aspect ratio and resolution. In *Proceedings of the Advances in Neural Information Processing Systems*, 2023. 3
- [12] Chaoyou Fu, Peixian Chen, Yunhang Shen, Yulei Qin, Mengdan Zhang, Xu Lin, Zhenyu Qiu, Wei Lin, Jinrui Yang, Xiawu Zheng, Ke Li, Xing Sun, and Rongrong Ji. MME: A comprehensive evaluation benchmark for multimodal large language models. *arXiv preprint arXiv:2306.13394*, 2023. 3, 6, 2, 4
- [13] Tianyu Fu, Tengxuan Liu, Qinghao Han, Guohao Dai, Shengen Yan, Huazhong Yang, Xuefei Ning, and Yu Wang. Framefusion: Combining similarity and importance for video token reduction on large visual language models. *arXiv preprint arXiv:2501.01986*, 2024. 1
- [14] Yash Goyal, Tejas Khot, Douglas Summers-Stay, Dhruv Batra, and Devi Parikh. Making the V in VQA matter: Elevating the role of image understanding in visual question answering. In *Proceedings of the IEEE/CVF Conference on Computer Vision and Pattern Recognition*, pages 6325–6334, 2017. 6
- [15] Danna Gurari, Qing Li, Abigale J. Stangl, Anhong Guo, Chi Lin, Kristen Grauman, Jiebo Luo, and Jeffrey P. Bigham. VizWiz grand challenge: Answering visual questions from blind people. In *Proceedings of the IEEE/CVF Conference on Computer Vision and Pattern Recognition*, pages 3608–3617, 2018. 6, 2
- [16] Yuhang Han, Xuyang Liu, Pengxiang Ding, Donglin Wang, Honggang Chen, Qingsen Yan, and Siteng Huang. Rethinking token reduction in mllms: Towards a unified paradigm for training-free acceleration. *arXiv preprint arXiv:2411.17686*, 2024. 1, 3, 4
- [17] Drew A. Hudson and Christopher D. Manning. GQA: A new dataset for real-world visual reasoning and compositional question answering. In *Proceedings of the IEEE/CVF Conference on Computer Vision and Pattern Recognition*, pages 6700–6709, 2019. 6, 2

- [18] Lei Jiang, Weizhe Huang, Tongxuan Liu, Yuting Zeng, Jing Li, Lechao Cheng, and Xiaohua Xu. Fopru: Focal pruning for efficient large vision-language models. *CoRR*, abs/2411.14164, 2024. 1
- [19] Aniruddha Kembhavi, Mike Salvato, Eric Kolve, Minjoon Seo, Hannaneh Hajishirzi, and Ali Farhadi. A diagram is worth a dozen images. In *Computer Vision—ECCV 2016: 14th European Conference, Amsterdam, The Netherlands, October 11–14, 2016, Proceedings, Part IV 14*, pages 235–251. Springer, 2016. 6, 2
- [20] Bohao Li, Yuying Ge, Yixiao Ge, Guangzhi Wang, Rui Wang, Ruimao Zhang, and Ying Shan. Seed-bench: Benchmarking multimodal large language models. In *Proceedings of the IEEE/CVF Conference on Computer Vision and Pattern Recognition*, pages 13299–13308, 2024. 6, 2
- [21] Bo Li, Yuanhan Zhang, Dong Guo, Renrui Zhang, Feng Li, Hao Zhang, Kaichen Zhang, Yanwei Li, Ziwei Liu, and Chunyuan Li. Llava-onevision: Easy visual task transfer. *arXiv preprint arXiv:2408.03326*, 2024. 3, 4, 6, 2
- [22] Junnan Li, Dongxu Li, Silvio Savarese, and Steven C. H. Hoi. BLIP-2: Bootstrapping language-image pre-training with frozen image encoders and large language models. In *Proceedings of the International Conference on Machine Learning*, pages 19730–19742, 2023. 2
- [23] Yifan Li, Yifan Du, Kun Zhou, Jinpeng Wang, Wayne Xin Zhao, and Ji-Rong Wen. Evaluating object hallucination in large vision-language models. In *Proceedings of the Conference on Empirical Methods in Natural Language Processing*, pages 292–305, 2023. 3, 2
- [24] Yanwei Li, Yuechen Zhang, Chengyao Wang, Zhisheng Zhong, Yixin Chen, Ruihang Chu, Shaoteng Liu, and Jiaya Jia. Mini-Gemini: Mining the potential of multi-modality vision language models. *arXiv preprint arXiv:2403.18814*, 2024. 1, 3
- [25] Youwei Liang, Chongjian Ge, Zhan Tong, Yibing Song, Jue Wang, and Pengtao Xie. Not all patches are what you need: Expediting vision transformers via token reorganizations. In *Proceedings of the International Conference on Learning Representations*, 2022. 3, 4
- [26] Zhihang Lin, Mingbao Lin, Luxi Lin, and Rongrong Ji. Boosting multimodal large language models with visual tokens withdrawal for rapid inference. *arXiv preprint arXiv:2405.05803*, 2024. 3
- [27] Haotian Liu, Chunyuan Li, Qingyang Wu, and Yong Jae Lee. Visual instruction tuning. In *Proceedings of the Advances in Neural Information Processing Systems*, 2023. 1
- [28] Haotian Liu, Chunyuan Li, Yuheng Li, and Yong Jae Lee. Improved baselines with visual instruction tuning. In *Proceedings of the IEEE/CVF Conference on Computer Vision and Pattern Recognition*, pages 26286–26296, 2024. 1, 2, 3
- [29] Haotian Liu, Chunyuan Li, Yuheng Li, Bo Li, Yuanhan Zhang, Sheng Shen, and Yong Jae Lee. LLaVA-NeXT: Improved reasoning, ocr, and world knowledge, 2024. 2, 3, 4, 6, 7
- [30] Haogeng Liu, Quanzeng You, Xiaotian Han, Yiqi Wang, Bohan Zhai, Yongfei Liu, Yunzhe Tao, Huaibo Huang, Ran He, and Hongxia Yang. InfiMM-HD: A leap forward in high-resolution multimodal understanding. *arXiv preprint arXiv:2403.01487*, 2024. 3
- [31] Ting Liu, Liangtao Shi, Richang Hong, Yue Hu, Quanjun Yin, and Linfeng Zhang. Multi-stage vision token dropping: Towards efficient multimodal large language model. *arXiv preprint arXiv:2411.10803*, 2024. 1
- [32] Yuan Liu, Haodong Duan, Yuanhan Zhang, Bo Li, Songyang Zhang, Wangbo Zhao, Yike Yuan, Jiaqi Wang, Conghui He, Ziwei Liu, Kai Chen, and Dahua Lin. MMBench: Is your multi-modal model an all-around player? In *Proceedings of the European Conference on Computer Vision*, pages 216–233, 2024. 3, 6, 2
- [33] Pan Lu, Swaroop Mishra, Tanglin Xia, Liang Qiu, Kai-Wei Chang, Song-Chun Zhu, Oyvind Tafjord, Peter Clark, and Ashwin Kalyan. Learn to explain: Multimodal reasoning via thought chains for science question answering. In *Proceedings of the Advances in Neural Information Processing Systems*, pages 2507–2521, 2022. 3, 6, 2
- [34] Gen Luo, Yiyi Zhou, Yuxin Zhang, Xiawu Zheng, Xiaoshuai Sun, and Rongrong Ji. Feast your eyes: Mixture-of-resolution adaptation for multimodal large language models. *arXiv preprint arXiv:2403.03003*, 2024. 3
- [35] OpenAI. GPT-4 technical report. *arXiv preprint arXiv:2303.08774*, 2023. 1
- [36] Alec Radford, Jong Wook Kim, Chris Hallacy, Aditya Ramesh, Gabriel Goh, Sandhini Agarwal, Girish Sastry, Amanda Askell, Pamela Mishkin, Jack Clark, Gretchen Krueger, and Ilya Sutskever. Learning transferable visual models from natural language supervision. In *Proceedings of the International Conference on Machine Learning*, pages 8748–8763, 2021. 3, 2
- [37] Yongming Rao, Wenliang Zhao, Benlin Liu, Jiwen Lu, Jie Zhou, and Cho-Jui Hsieh. DynamicViT: Efficient vision transformers with dynamic token sparsification. In *Proceedings of the Advances in Neural Information Processing Systems*, pages 13937–13949, 2021. 3
- [38] Yuzhang Shang, Mu Cai, Bingxin Xu, Yong Jae Lee, and Yan Yan. LLaVA-PruMerge: Adaptive token reduction for efficient large multimodal models. *arXiv preprint arXiv:2403.15388*, 2024. 1, 3
- [39] Amanpreet Singh, Vivek Natarajan, Meet Shah, Yu Jiang, Xinlei Chen, Dhruv Batra, Devi Parikh, and Marcus Rohrbach. Towards VQA models that can read. In *Proceedings of the IEEE/CVF Conference on Computer Vision and Pattern Recognition*, pages 8317–8326, 2019. 3, 6, 2
- [40] Hugo Touvron, Thibaut Lavril, Gautier Izacard, Xavier Martinet, Marie-Anne Lachaux, Timothée Lacroix, Baptiste Rozière, Naman Goyal, Eric Hambro, Faisal Azhar, Aurélien Rodriguez, Armand Joulin, Edouard Grave, and Guillaume Lample. LLaMA: Open and efficient foundation language models. *arXiv preprint arXiv:2302.13971*, 2023. 1
- [41] Ashish Vaswani, Noam Shazeer, Niki Parmar, Jakob Uszkoreit, Llion Jones, Aidan N Gomez, Łukasz Kaiser, and Illia Polosukhin. Attention is all you need. In *Proceedings of the Advances in Neural Information Processing Systems*, pages 5998–6008, 2017. 4
- [42] Peng Wang, Shuai Bai, Sinan Tan, Shijie Wang, Zhihao Fan, Jinze Bai, Keqin Chen, Xuejing Liu, Jialin Wang, Wenbin

- Ge, Yang Fan, Kai Dang, Mengfei Du, Xuancheng Ren, Rui Men, Dayiheng Liu, Chang Zhou, Jingren Zhou, and Junyang Lin. Qwen2-VL: Enhancing vision-language model’s perception of the world at any resolution. *arXiv preprint arXiv:2409.12191*, 2024. 3
- [43] JingJing Xie, Yuxin Zhang, Mingbao Lin, Liujuan Cao, and Rongrong Ji. Advancing multimodal large language models with quantization-aware scale learning for efficient adaptation. In *Proceedings of the ACM International Conference on Multimedia*, 2024. 1
- [44] An Yang, Baosong Yang, Binyuan Hui, Bo Zheng, Bowen Yu, Chang Zhou, Chengpeng Li, Chengyuan Li, Dayiheng Liu, Fei Huang, Guanting Dong, Haoran Wei, Huan Lin, Jialong Tang, Jialin Wang, Jian Yang, Jianhong Tu, Jianwei Zhang, Jianxin Ma, Jianxin Yang, Jin Xu, Jingren Zhou, Jinze Bai, Jinzheng He, Junyang Lin, Kai Dang, Keming Lu, Keqin Chen, Kexin Yang, Mei Li, Mingfeng Xue, Na Ni, Pei Zhang, Peng Wang, Ru Peng, Rui Men, Ruize Gao, Runji Lin, Shijie Wang, Shuai Bai, Sinan Tan, Tianhang Zhu, Tianhao Li, Tianyu Liu, Wenbin Ge, Xiaodong Deng, Xiaohuan Zhou, Xingzhang Ren, Xinyu Zhang, Xipin Wei, Xuancheng Ren, Xuejing Liu, Yang Fan, Yang Yao, Yichang Zhang, Yu Wan, Yunfei Chu, Yuqiong Liu, Zeyu Cui, Zhenru Zhang, Zhifang Guo, and Zhihao Fan. Qwen2 technical report, 2024. 2, 3
- [45] Senqiao Yang, Yukang Chen, Zhuotao Tian, Chengyao Wang, Jingyao Li, Bei Yu, and Jiaya Jia. Visionzip: Longer is better but not necessary in vision language models. *arXiv preprint arXiv:2412.04467*, 2024. 3
- [46] Weihao Ye, Qiong Wu, Weihao Lin, and Yiyi Zhou. Fit and prune: Fast and training-free visual token pruning for multi-modal large language models. *arXiv preprint arXiv:2409.10197*, 2024. 3
- [47] Xubing Ye, Yukang Gan, Xiaoke Huang, Yixiao Ge, Ying Shan, and Yansong Tang. VoCo-LLaMA: Towards vision compression with large language models. *arXiv preprint arXiv:2406.12275*, 2024. 1
- [48] Weihao Yu, Zhengyuan Yang, Linjie Li, Jianfeng Wang, Kevin Lin, Zicheng Liu, Xinchao Wang, and Lijuan Wang. MM-Vet: Evaluating large multimodal models for integrated capabilities. In *Proceedings of the International Conference on Machine Learning*, 2024. 3, 6, 2
- [49] Zhihang Yuan, Yuzhang Shang, Yang Zhou, Zhen Dong, Zhe Zhou, Chenhao Xue, Bingzhe Wu, Zhikai Li, Qingyi Gu, Yong Jae Lee, Yan Yan, Beidi Chen, Guangyu Sun, and Kurt Keutzer. LLM inference unveiled: Survey and roofline model insights. *arXiv preprint arXiv:2402.16363*, 2024. 3
- [50] Xiaohua Zhai, Basil Mustafa, Alexander Kolesnikov, and Lucas Beyer. Sigmoid loss for language image pre-training. In *Proceedings of the IEEE/CVF International Conference on Computer Vision*, pages 11941–11952, 2023. 6, 1, 2
- [51] Hang Zhang, Xin Li, and Lidong Bing. Video-LLaMA: An instruction-tuned audio-visual language model for video understanding. In *Proceedings of the Conference on Empirical Methods in Natural Language Processing*, pages 543–553, 2023. 1
- [52] Qizhe Zhang, Aosong Cheng, Ming Lu, Zhiyong Zhuo, Minqi Wang, Jiajun Cao, Shaobo Guo, Qi She, and Shanghang Zhang. [CLS] attention is all you need for training-free visual token pruning: Make vlm inference faster. *arXiv preprint arXiv:2412.01818*, 2024. 1, 3, 6, 7, 8, 2
- [53] Yuan Zhang, Chun-Kai Fan, Junpeng Ma, Wenzhao Zheng, Tao Huang, Kuan Cheng, Denis Gudovskiy, Tomoyuki Okuno, Yohei Nakata, Kurt Keutzer, and Shanghang Zhang. SparseVLM: Visual token sparsification for efficient vision-language model inference. *arXiv preprint arXiv:2410.04417*, 2024. 1, 3, 6, 7, 2

Global Compression Commander: Plug-and-Play Inference Acceleration for High-Resolution Large Vision-Language Models

Supplementary Material

In the appendix, we provide theoretical FLOPs calculation in Section 7, more discussions about GlobalCom² without [CLS] token in Section 8, detailed benchmarks introduction and implementation details in Section 9, more additional experiments and analysis in Section 10, and detailed explanation of our GlobalCom² in Section 11.

7. Theoretical Complexity Analysis

GlobalCom² compresses a large number of visual tokens for HR-LVLMs, thereby reducing their computational costs. Below, we analyze the theoretical computational complexity of HR-LVLMs in both the prefill stage and the decoding stage.

During the prefill stage, the FLOPs for a single transformer layer can be estimated using the formula $8Td^2 + 4T^2d + 6Tdm$. When applying a token retention ratio R , where the retained token count is defined as $\hat{T} = R \cdot T$, the corresponding theoretical FLOPs reduction ratio η can be reformulated to account for this adjustment:

$$\begin{aligned} \eta &= 1 - \frac{8\hat{T}d^2 + 4\hat{T}^2d + 6\hat{T}dm}{8Td^2 + 4T^2d + 6Tdm} \\ &= 1 - \frac{R(8d + 4RT + 6m)}{8d + 4T + 6m} \end{aligned} \quad (8)$$

In the decoding stage, the integration of a KV-Cache substantially enhances computational efficiency. This improvement is evidenced by the reduction in the complexity of attention computation to $\mathcal{O}(T)$. As a result, the formula for computing FLOPs is refined to $8d^2 + 4Td + 6Tdm$. Given the current limitations of hardware, managing dynamic KV-Cache lengths effectively during the inference process presents significant challenges. Therefore, implementing pruning strategies prior to the decoder in large language models could facilitate a more efficient acceleration of the inference process.

8. More Discussions about Token Evaluation without [CLS].

Some Vision Encoders like SigLIP [50] do not own [CLS] tokens, rendering existing token compression methods that rely on [CLS] tokens (e.g., FasterVLM [52]) ineffective. Therefore, we explore alternative token importance evaluation approaches for such encoders. This enables GlobalCom² to measure information content in each crop

and adaptively allocate token budgets, preserving tokens with higher **information richness**.

As visualized in Figure 9, we first examine the attention patterns of CLIP-ViT’s final layer [CLS] token as a baseline for evaluating alternative token importance assessment strategies. We explore two approaches to measure token information without relying on [CLS] token:

(a) Patch Attention Analysis: We calculate each patch token’s importance by averaging its attention scores with all other patch tokens:

$$a_i = \frac{1}{N-1} \sum_{j \neq i} A_{i,j}, \quad (9)$$

where $A_{i,j}$ denotes the attention score from token i to token j , and N is the total number of patch tokens. Interestingly, as shown in the “Patch Attention” visualization in Figure 9, tokens with high informativeness exhibit **lower** average attention scores. This aligns with the intuition that tokens heavily attending to other tokens (high average attention scores) are more likely to be replaceable, as they primarily aggregate information from their neighbors. Conversely, tokens with low average attention scores tend to be more unique and irreplaceable, containing distinct information vital for image understanding. By negating these scores (shown as “Negative Patch Attention”), we obtain patterns that relatively align with [CLS]-based assessment.

(b) Global Mean Similarity: We compute a global mean vector $\mathbf{g} \in \mathbb{R}^d$ through *global average pooling* over all tokens, then calculate the cosine similarity between each patch token \mathbf{x}_i and \mathbf{g} :

$$c_i = \cos(\mathbf{x}_i, \mathbf{g}) = \frac{\mathbf{x}_i \cdot \mathbf{g}}{\|\mathbf{x}_i\| \|\mathbf{g}\|}, \quad (10)$$

Tokens with low similarity to \mathbf{g} typically represent **distinctive** visual elements that *deviate* from the average representation, suggesting their **irreplaceability** in capturing unique semantic information. Conversely, tokens highly similar to \mathbf{g} often correspond to common or repetitive patterns, indicating their redundancy in visual representation. The “Negative Similarity with token \mathbf{g} ” visualization aligns well with [CLS]-based assessment, highlighting semantically rich regions like the baseball player in the top-right example of Figure 9.

Based on these observations, we define two token importance measures:

$$s_i^{attn} = -a_i, \quad s_i^{sim} = -c_i, \quad (11)$$

where s_i^{attn} represents the “Negative Patch Attention”

Method	VQA ^T	POPE	MME	MM-Vet	MMBSQA	Avg.
<i>Upper Bound, 2880 Tokens</i>						
Vanilla	64.9	86.5	1519.0	43.9	67.4	70.1 100.0%
<i>Ratio=25%, Retain up to 720 Tokens</i>						
$s_i^{[CLS]}$	60.9	87.6	1493.5	39.5	65.9	68.1 96.4%
s_i^{attn}	58.7	85.7	1449.3	36.6	63.5	67.9 93.2%
s_i^{sim}	60.3	87.3	1485.8	39.7	65.0	67.6 95.8%

Table 5. Effects of different token evaluation metrics.

score and s_i^{sim} denotes the ‘‘Negative Similarity’’ score. Both scores are designed to highlight informative tokens: s_i^{attn} identifies tokens that maintain their distinctiveness by less attending to others, while s_i^{sim} emphasizes tokens that deviate from the average representation \mathbf{g} . These measures serve as effective alternatives to $[CLS]$ -based assessment (denoted as $s_i^{[CLS]}$) in our quantitative experiments.

Table 5 compares the effectiveness of $s_i^{[CLS]}$, s_i^{attn} , and s_i^{sim} when used as metrics for both *adaptive compression adjustment* and *holistic token evaluation* in GlobalCom². While all three measures help preserve informative visual tokens to some extent, s_i^{attn} shows notably different behavior from the other two metrics. Notably, s_i^{sim} demonstrates performance closest to $s_i^{[CLS]}$ across various benchmarks, even outperforming it on MM-Vet. Based on these results, we adopt s_i^{sim} as an alternative to $s_i^{[CLS]}$ for measuring information content of local crops and visual tokens when $[CLS]$ token is unavailable, enabling training-free token compression for HR-LVLMs.

9. Detailed Experimental Settings

Benchmark Details. We evaluate GlobalCom² on various multimodal understanding benchmarks detailed as follows:

- **GQA** [17]: Contains 113,018 real-world images with scene graphs for structured visual reasoning.
- **VizWiz** [15]: Features over 39,000 questions from blind users with lower-quality images and conversational style.
- **SQA** [33]: Contains 21,000 scientific questions covering 26 topics and 379 different reasoning skills.
- **VQA^T** [39]: Features 28,000 images focusing on comprehension of text embedded in natural scenes.
- **AI2D** [19]: Contains 5,000 high-resolution scientific diagrams paired with visual-spatial reasoning questions.
- **MMStar** [7]: Contains 12,000 high-resolution images for spatial, temporal, and commonsense reasoning.
- **POPE** [23]: Features 14,000 images with binary questions for detecting object hallucination phenomena.
- **MME** [12]: Contains 15,000 images across 14 perceptual and cognitive reasoning subtasks.
- **MMB** [32]: Features 20,000 multiple-choice questions designed for robust visual reasoning.
- **MMBCN** [32]: Chinese counterpart of MMB with 20,000 questions for cross-lingual evaluation.

- **MM-Vet** [48]: Features 16,000 questions across recognition, OCR, knowledge, and spatial reasoning.
- **SEED-Bench** [20]: Contains 19,000 human-annotated questions across 12 evaluation dimensions.

Baseline Models. We select LLaVA-NeXT [29] and LLaVA-OneVision (SI) [21] as our baseline models, and follow the same inference setting as the original paper as it is publicly available¹. LLaVA-NeXT and LLaVA-OneVision share a common three-component architecture: a pre-trained vision encoder, a large language model (LLM) backbone, and a two-layer MLP projector bridging the two. Specifically, LLaVA-NeXT employs CLIP-ViT-L-336px [36] and Vicuna-v1.5 for vision and language modeling respectively, while LLaVA-OneVision utilizes SigLIP-So400m-Patch14-384 [50] and Qwen2 [44]. To effectively process high-resolution visual inputs, both models adopt flexible grid configurations - LLaVA-NeXT supports $\{2 \times 2, 1 \times \{2, 3, 4\}, \{2, 3, 4\} \times 1\}$ with maximum 5×576 grid tokens, while LLaVA-OneVision allows $\{1 \times 1, \dots, 6 \times 6\}$ grids up to 10×729 tokens.

Comparison Methods. We compare our GlobalCom² with three dominant baseline methods:

- **FastV** [8] performs one-time token pruning after the selected layer of LLM based on attention map analysis.
- **SparseVLM** [53] ranks token importance by text-visual attention maps, pruning through pre-selected text prompts to reduce attention noise.
- **FasterVLM** [52] reranks visual tokens by $[CLS]$ attention scores from CLIP-ViT and preserves top- k tokens.

All experiments are conducted on NVIDIA A100-SXM4-80GB GPUs.

10. Additional Experiments

10.1. Comparisons on LLaVA-NeXT-13B.

Considering that both FasterVLM and GlobalCom² perform token compression at the vision encoding stage, Table 6 focuses on comparing these two methods. The results reveal several key findings: **(1)** Our GlobalCom² outperforms FasterVLM on most benchmarks, maintaining **above 90%** of uncompressed performance across different retention ratios on both LLaVA-NeXT-7B and 13B models. **(2)** On visual text understanding (VQA^T), GlobalCom² shows particular strength at low retention ratios, surpassing FasterVLM by 2.6% at $R = 10\%$, thanks to its effective preservation of object and textual information. **(3)** While FasterVLM performs slightly better on general visual tasks (VQAv2, MMB, MMBCN) at high retention ratios due to its uniform token compression, GlobalCom² demonstrates

¹LLaVA-NeXT: <https://github.com/haotian-liu/LLaVA/blob/main/docs/Evaluation.md>, LLaVA-OneVision: https://github.com/LLaVA-VL/LLaVA-NeXT/blob/main/docs/LLaVA_OneVision.md.

Method	VQAv2	GQA	VizWiz	SQA	VQA ^T	POPE	MME	MMB	MMBCN	MM-Vet	Average
<i>Upper Bound, 2880 Tokens</i>											
LLaVA-NeXT-13B [29]	82.8	65.4	60.5	73.5	67.1	86.2	1575.9	70.0	64.2	48.4	100.0%
<i>Ratio=75%, Retain up to 2160 Tokens</i>											
FasterVLM [52]	81.9	64.6	58.7	72.6	62.8	87.6	1560.3	69.8	64.8	47.5	98.7%
GlobalCom²	81.9	65.0	58.6	72.8	65.2	87.8	1567.9	69.2	64.7	49.6	99.5%
<i>Ratio=50%, Retain up to 1440 Tokens</i>											
FasterVLM [52]	81.3	64.2	57.0	72.5	62.4	87.6	1534.1	69.5	64.1	44.7	97.3%
GlobalCom²	81.0	64.7	57.1	73.2	64.6	87.7	1553.5	69.3	63.5	48.0	98.4%
<i>Ratio=25%, Retain up to 720 Tokens</i>											
FasterVLM [52]	78.9	62.3	55.0	72.1	61.2	86.1	1516.1	67.6	62.1	44.6	95.2%
GlobalCom²	79.9	62.7	55.1	72.3	63.6	86.5	1531.2	67.9	62.2	43.5	95.8%
<i>Ratio=10%, Retain up to 288 Tokens</i>											
FasterVLM [52]	74.5	58.1	52.8	70.5	58.0	81.6	1386.2	61.7	53.5	38.3	88.2%
GlobalCom²	77.0	58.3	52.5	71.8	60.3	82.4	1399.5	65.0	58.5	37.9	90.3%

Table 6. Comparison with other training-free LVLM token compression methods with LLaVA-NeXT-13B across 10 benchmarks.

Method	GQA	VizWiz	SQA	AI2D	MMStar	MME	SEED	Avg.
<i>Upper Bound, 7290 Tokens</i>								
LLaVA-OV	59.5	46.0	67.9	54.2	36.2	1216.1	63.8	100.0%
$R = 75\%$	58.9	44.5	67.9	52.7	37.1	1205.3	63.3	99.1%
$R = 50\%$	57.4	44.3	67.6	52.0	37.0	1216.1	62.6	98.4%
$R = 25\%$	54.2	42.1	67.0	51.3	35.8	1201.8	60.4	95.4%
$R = 15\%$	50.6	41.0	67.5	50.4	35.4	1140.2	56.8	91.1%
$R = 10\%$	48.6	40.7	67.1	50.0	35.0	1085.7	54.9	90.5%

Table 7. Results of adopting GlobalCom² on LLaVA-OV-0.5B.

superior degradation resistance at low ratios. For example, when R drops from 25% to 10%, FasterVLM’s performance significantly decreases by 5.9% and 8.6% on MMB and MMBCN, while GlobalCom² only drops by 2.9% and 3.7%, benefiting from our carefully designed global view-guided compression strategy.

10.2. Results on LLaVA-OneVision-0.5B.

We adopt s_i^{sim} proposed in Section 8 as the measure for crop information richness and token informativeness, and evaluate our GlobalCom² on the LLaVA-OneVision model with more local crops across multiple benchmarks.

Our experimental results show that GlobalCom² maintains satisfactory performance even under low retention ratios ($R = 25\%, 15\%, 10\%$). Particularly, GlobalCom² achieves promising results on AI2D and MMStar benchmarks which involve high-resolution images. Interestingly, we observe that on the SQA benchmark, the model performance shows minimal degradation as token retention rate decreases. We attribute this to SQA’s lower dependency on visual signals and higher reliance on LLM capabilities. Given that LLaVA-OneVision employs the powerful Qwen2 [44] as its LLM decoder, it consistently performs well on this benchmark regardless of retention ratio.

10.3. Sensitivity Analysis of Hyper-parameters.

We further explore the hyper-parameter configurations τ and α of our GlobalCom² in Figure 7.

Hyper-parameter τ serves as the temperature in the softmax function when assessing local crop significance, controlling the “sharpness” of probability distribution. A smaller τ leads to a sharper distribution, amplifying the differences in global visual importance among local crops. As shown in the first row of Figure 7, our GlobalCom² demonstrates robust performance across most benchmarks, particularly on VQA^T [39] and POPE [23], with varying τ validating our design principle for HR-LVLMs of allocating retention ratios based on each local crop’s global importance. We empirically set $\tau = 10$ to achieve optimal performance across most benchmarks.

Hyper-parameter α determines the criterion for token retention in local crops, where a larger α indicates stronger dependence on global guidance for token retention in local crops. Similar to τ , the second row of Figure 7 shows that our GlobalCom² exhibits consistent effectiveness across most benchmarks under different α settings, substantiating our dual-perspective token retention strategy of local crops by considering their significance at both global and local levels for HR-LVLMs.

10.4. Detailed Efficiency Analysis.

We conduct a comprehensive analysis of both theoretical and practical efficiency of our GlobalCom² with LLaVA-NeXT-7B/13B on a single NVIDIA A100-SXM4-80GB GPU, as shown in Table 8 and Table 9. We measure computational efficiency using TFLOPs and peak memory consumption directly, while other metrics are estimated using LLM-Viewer [49]. Given that the sequence length of visual tokens substantially exceeds that of textual and system tokens, we *exclude* the latter two from our theoretical anal-

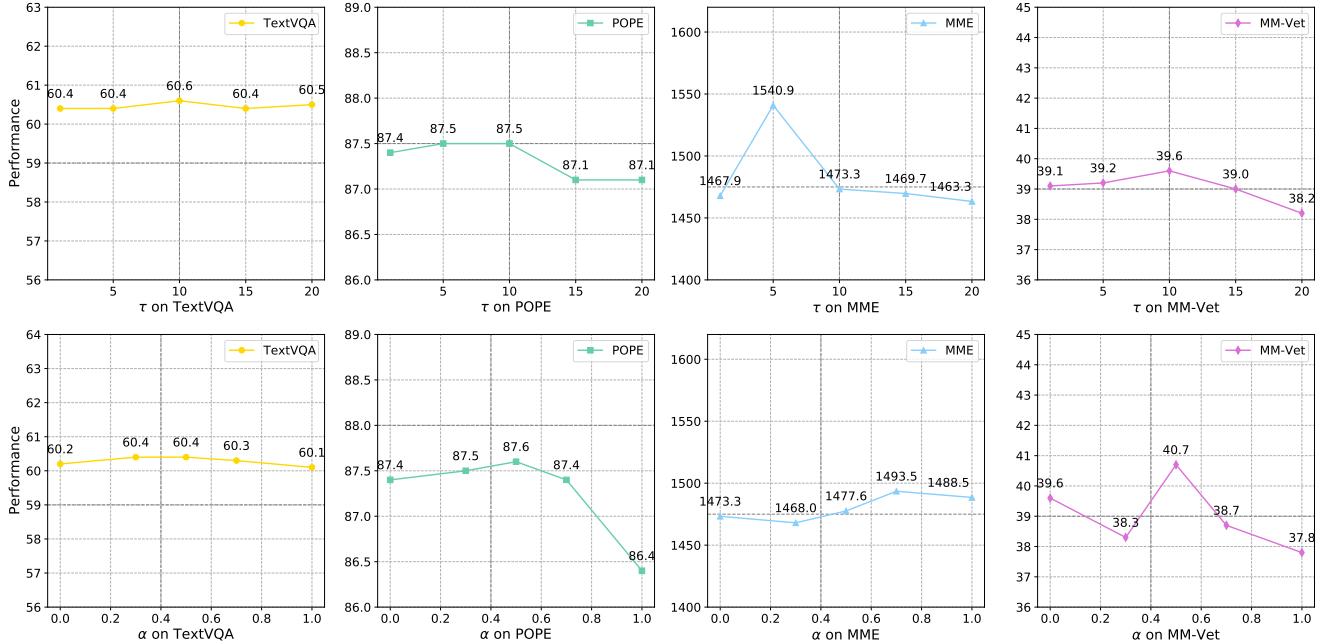


Figure 7. **Hyper-parameter sensitivity analysis of τ and α .** Hyper-parameter τ controls the sharpness of probability distribution in softmax when assessing local crop informativeness, while hyper-parameter α determines the token retention threshold where higher values indicate stronger reliance on global guidance.

Method	TFLOPs \downarrow	Peak Memory (GB) \downarrow	KV-Cache (MB) \downarrow	Prefill Time (ms) \downarrow	Throughput (samples/s) \uparrow	Performance \uparrow
<i>Upper Bound, 2880 Tokens</i>						
LLaVA-NeXT-7B	41.7	23.8	1536.0	170.7	2.5	1519.0
<i>Ratio=75%, Retain up to 2160 Tokens</i>						
GlobalCom²	30.4 ($\downarrow 27\%$)	17.8 ($\downarrow 25\%$)	1126.4 ($\downarrow 27\%$)	119.9 ($\downarrow 30\%$)	3.2 (1.3 \times)	1548.4
<i>Ratio=50%, Retain up to 1440 Tokens</i>						
GlobalCom²	19.7 ($\downarrow 53\%$)	16.2 ($\downarrow 32\%$)	755.0 ($\downarrow 51\%$)	74.5 ($\downarrow 57\%$)	4.2 (1.7 \times)	1552.9
<i>Ratio=25%, Retain up to 720 Tokens</i>						
GlobalCom²	9.6 ($\downarrow 77\%$)	14.8 ($\downarrow 39\%$)	377.0 ($\downarrow 76\%$)	34.6 ($\downarrow 80\%$)	5.3 (2.1 \times)	1493.5
<i>Ratio=10%, Retain up to 288 Tokens</i>						
GlobalCom²	3.8 ($\downarrow 91\%$)	14.2 ($\downarrow 40\%$)	151.0 ($\downarrow 90\%$)	13.3 ($\downarrow 92\%$)	6.8 (2.7 \times)	1365.5

Table 8. **Efficiency analysis of our GlobalCom² with LLaVA-NeXT-7B on one NVIDIA A100-SXM4-80GB GPU.**

Method	TFLOPs \downarrow	Peak Memory (GB) \downarrow	KV-Cache (MB) \downarrow	Prefill Time (ms) \downarrow	Throughput (samples/s) \uparrow	Performance \uparrow
<i>Upper Bound, 2880 Tokens</i>						
LLaVA-NeXT-13B	80.0	36.7	2457.6	295.1	1.9	1575.9
<i>Ratio=75%, Retain up to 2160 Tokens</i>						
GlobalCom²	58.7 ($\downarrow 27\%$)	34.1 ($\downarrow 7\%$)	1843.2 ($\downarrow 25\%$)	211.6 ($\downarrow 28\%$)	2.4 (1.3 \times)	1567.9
<i>Ratio=50%, Retain up to 1440 Tokens</i>						
GlobalCom²	38.3 ($\downarrow 52\%$)	30.1 ($\downarrow 18\%$)	1228.8 ($\downarrow 50\%$)	134.6 ($\downarrow 54\%$)	3.2 (1.7 \times)	1553.5
<i>Ratio=25%, Retain up to 720 Tokens</i>						
GlobalCom²	18.7 ($\downarrow 77\%$)	27.5 ($\downarrow 25\%$)	590.0 ($\downarrow 76\%$)	64.1 ($\downarrow 78\%$)	4.8 (2.4 \times)	1531.2
<i>Ratio=10%, Retain up to 288 Tokens</i>						
GlobalCom²	7.4 ($\downarrow 91\%$)	26.2 ($\downarrow 29\%$)	236.0 ($\downarrow 90\%$)	25.0 ($\downarrow 92\%$)	5.8 (3.1 \times)	1399.5

Table 9. **Efficiency analysis of our GlobalCom² with LLaVA-NeXT-13B on one NVIDIA A100-SXM4-80GB GPU.**

ysis. For practical efficiency, “Throughput” and the corresponding “Performance” measurements are conducted on the MME benchmark [12], which includes 2374 examples.

As shown in Table 8 and Table 9, GlobalCom² substantially improves the computational efficiency of LLaVA-NeXT models across both theoretical and practical metrics. Specifically, while preserving model performance,

our method achieves significant reductions in GPU memory consumption and notable acceleration in inference speed compared to the original LLaVA-NeXT. Most importantly, these efficiency improvements are achieved through a training-free compression scheme, demonstrating the immediate practical value of GlobalCom².

10.5. More Visualizations of Token Compression

In Figure 8, we present more token compression visualizations of GlobalCom². It is clear that in all cases, *entity-rich* regions are effectively preserved while redundant ones are removed. For crops with high visual redundancy (*e.g.*, the camera’s golden casing in the top-right case), it applies aggressive compression ($r_4 = 19\%$). Conversely, for semantically dense regions (*e.g.*, the text-rich first crop in the top-right case), it maintains more tokens ($r_1 = 43\%$) to ensure detailed understanding. More cases in Appendix 8 further demonstrate GlobalCom²’s consistent ability to adaptively preserve significant regions while removing redundancy at both global and local views.

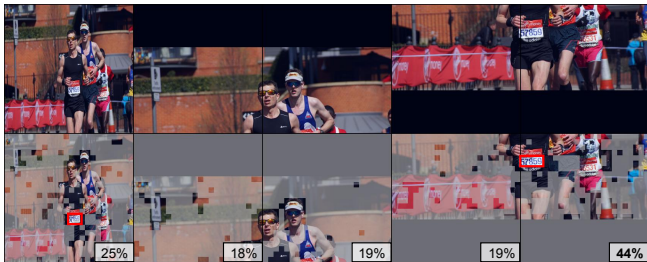
11. Algorithm Illustration

We present a comprehensive description of GlobalCom² token compression for both global thumbnail and local crops in Algorithm 1 and Algorithm 2, respectively.

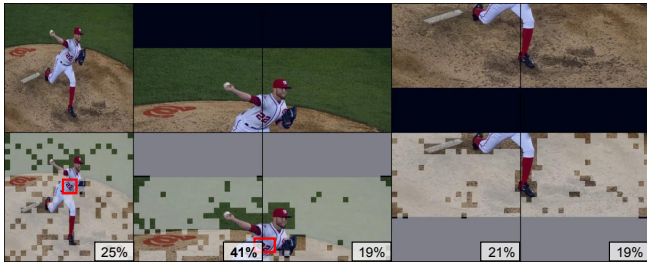
Q1: "What football league is the jacket from on the man pointing?"
 A1: "Ryman"



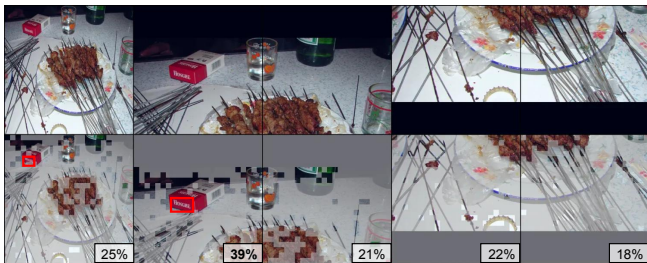
Q3: "What is the number of the runner in the lead right now?"
 A3: "57859"



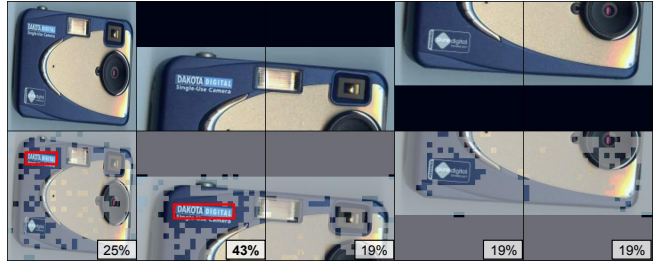
Q5: "What number is on the player's jersey?"
 A5: "22"



Q7: "What are the brand of cigarettes?"
 A7: "Honghe"



Q2: "What is the brand of this camera?"
 A2: "DAKOTA DIGITAL"



Q4: "What time is on the clock?"
 A4: "15:08:25"



Q6: "Was the ruler made in 2002?"
 A6: "Yes"



Q8: "What number is the player looking at the children?"
 A8: "9"



Figure 8. More visualization of token compression by GlobalCom². The presented examples are from VQA^T, where grey masks indicate discarded visual tokens.

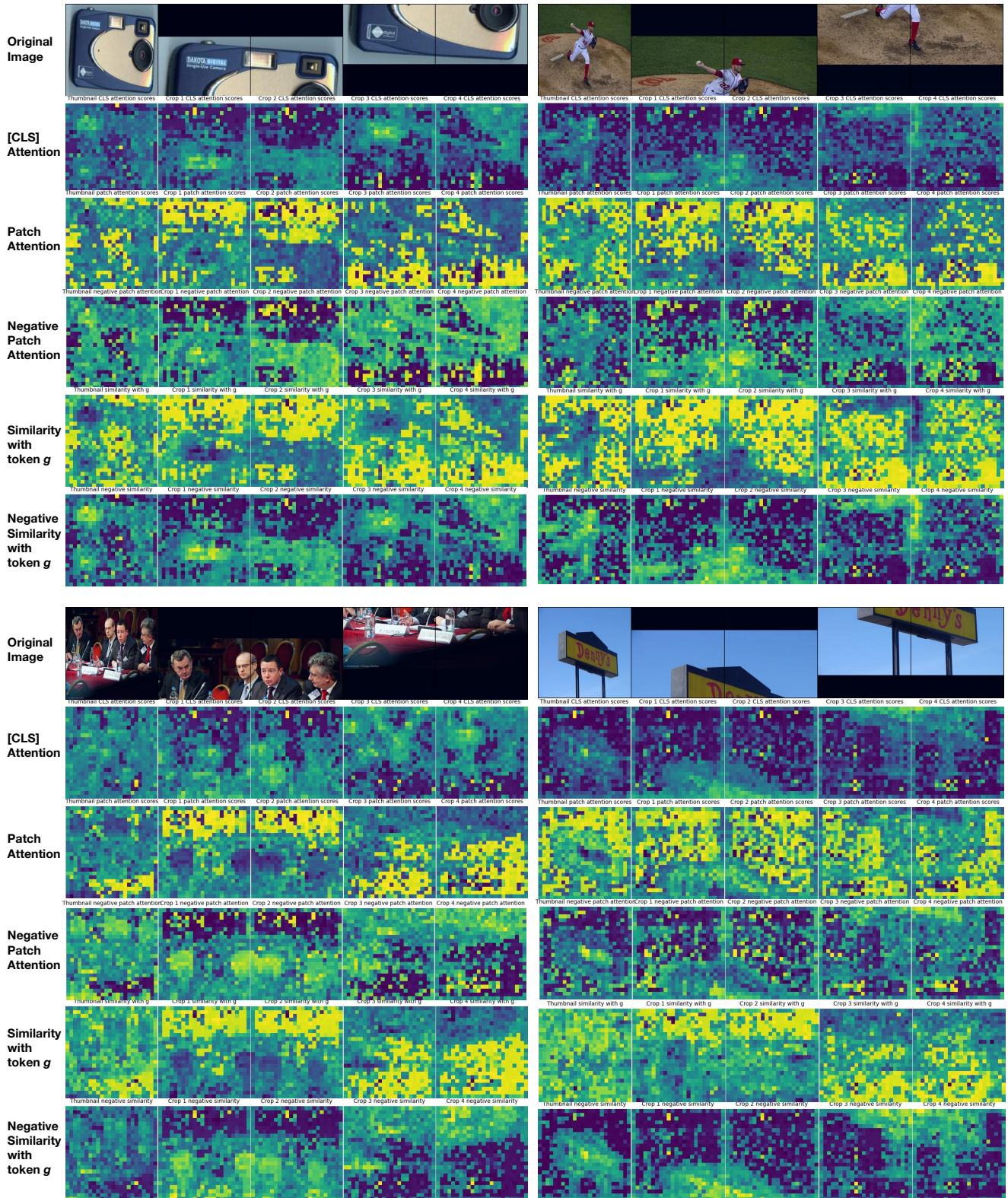


Figure 9. Visualization of different token evaluation scores.

Algorithm 1 GlobalCom²: Thumbnail Compression

Require: Global thumbnail tokens $\mathbf{X}^G \in \mathbb{R}^{N \times D}$, Vision encoder, Preset retention ratio $R \in (0, 1]$

Ensure: Compressed tokens $\hat{\mathbf{X}}^G \in \mathbb{R}^{k \times D}$ ($k = R \cdot N$)

- 1: // For models with [CLS] token
- 2: **if** model has [CLS] token **then**
- 3: Get [CLS] query \mathbf{q}^{CLS} and Key matrix \mathbf{K}
- 4: Compute importance scores:

$$s_i^G \leftarrow \frac{\exp(\mathbf{q}^{\text{CLS}} \mathbf{K}_i^\top / \sqrt{D})}{\sum_{j=1}^N \exp(\mathbf{q}^{\text{CLS}} \mathbf{K}_j^\top / \sqrt{D})}, \forall i$$

- 5: **else**
- 6: // For models without [CLS] token
- 7: Compute global mean vector: $\mathbf{g} \leftarrow \frac{1}{N} \sum_{i=1}^N \mathbf{x}_i$
- 8: Compute cosine similarity scores:

$$s_i^G \leftarrow -\frac{\mathbf{x}_i \cdot \mathbf{g}}{\|\mathbf{x}_i\| \|\mathbf{g}\|}, \forall i$$

- 9: **end if**
 - 10: Sort indices: $\text{idx} \leftarrow \text{argsort}([s_1^G, \dots, s_N^G])$ (descending)
 - 11: Retain top- k tokens: $\hat{\mathbf{X}}^G \leftarrow \mathbf{X}^G[\text{idx}[1 : k]]$
 - 12: **return** $\hat{\mathbf{X}}^G$
-

Algorithm 2 GlobalCom²: Local Crop Compression

Require: Local crops $\{\mathbf{X}_j^L\}_{j=1}^n$, Global importance scores s^G , Preset retention ratio R , Balance weight α , Temperature τ

Ensure: Compressed crop tokens $\{\hat{\mathbf{X}}_j^L\}_{j=1}^n$

- 1: **Adaptive Compression Adjustment:**
- 2: **for** each crop $j \in [1, n]$ **do**
- 3: Compute information richness:

$$s_j^G \leftarrow \sum_{i \in \text{crop}_j} s_i^G$$

- 4: Normalize: $\tilde{s}_j \leftarrow (s_j^G - \max\{s_j^G\})/\tau$
- 5: **end for**
- 6: Compute importance weights:

$$\sigma_j \leftarrow \frac{\exp(\tilde{s}_j)}{\sum_{l=1}^n \exp(\tilde{s}_l) + \epsilon}$$

- 7: Adjust retention ratios:

$$r_j \leftarrow R \times (1 + \sigma_j - \frac{1}{n})$$

- 8: **Holistic Token Evaluation:**

- 9: **for** each crop $j \in [1, n]$ **do**
 - 10: Compute local scores s_j^L via vision encoder
 - 11: Get global sub-scores \hat{s}_j^G via interpolation
 - 12: L2-normalize both s_j^L and \hat{s}_j^G
 - 13: Combine scores: $s_{j,i} \leftarrow \alpha \hat{s}_{j,i}^G + (1 - \alpha) s_{j,i}^L$
 - 14: Compress: $\hat{\mathbf{X}}_j^L \leftarrow \text{TopK}(\mathbf{X}_j^L, s_{j,i}, r_j \times N)$
 - 15: **end for**
 - 16: **return** $\{\hat{\mathbf{X}}_j^L\}_{j=1}^n$
-